ELSEVIER

Sensors and Actuators A 94 (2001) 177–188

SENSORS AND ACTUATORS A PHYSICAL

www.elsevier.com/locate/sna

High-cycle fatigue and durability of polycrystalline silicon thin films in ambient air

C.L. Muhlstein[a,*], S.B. Brown[b], R.O. Ritchie[a]

[a]Department of Materials Science and Engineering, University of California, LBNL, 1 Cyclotron Road, MS 62-203, Berkeley, CA 94720-1760, USA

[b]Exponent Incorporated, Natick, MA 01760, USA

Received 17 April 2001; received in revised form 28 July 2001; accepted 3 August 2001

Abstract

To evaluate the long-term durability properties of materials for microelectromechanical systems (MEMS), the stress-life (*S/N*) cyclic fatigue behavior of a 2-μm thick polycrystalline silicon film was evaluated in laboratory air using an electrostatically actuated notched cantilever beam resonator. A total of 28 specimens were tested for failure under high frequency (~40 kHz) cyclic loads with lives ranging from about 10 s to 34 days (3×10^5 to 1.2×10^{11} cycles) over fully reversed, sinusoidal stress amplitudes varying from ~2.0 to 4.0 GPa. The thin-film polycrystalline silicon cantilever beams exhibited a time-delayed failure that was accompanied by a continuous increase in the compliance of the specimen. This apparent cyclic fatigue effect resulted in an endurance strength, at greater than 10^9 cycles, of ~2 GPa, i.e. roughly one-half of the (single cycle) fracture strength. Based on experimental and numerical results, the fatigue process is attributed to a novel mechanism involving the environmentally-assisted cracking of the surface oxide film (termed reaction-layer fatigue). These results provide the most comprehensive, high-cycle, endurance data for designers of polysilicon micromechanical components available to date.
© 2001 Elsevier Science B.V. All rights reserved.

Keywords: Fatigue; Stress-life; Durability; Silicon; Polysilicon; MEMS

1. Introduction

Over the past decade, microelectromechanical systems (MEMS) and the enabling technologies of surface micromachining have evolved from academic laboratory exercises to established commercial fabrication strategies. During this period of rapid innovation, a vast array of MEMS applications have emerged and commercial products have entered the marketplace. These applications range from memory, mass storage and display applications for personal computing to critical sensor applications such as pressure transducers in medical devices and inertial sensors for passive restraint systems (e.g. airbags) and active automotive suspensions. Two-key points have become clear as MEMS are emerging from their infancy. First, silicon-based films are still the dominant structural material for micromachines. Second, the reliability of these components is critical for both product performance and safeguarding human life. Consequently, studies that characterize the failure modes that will ultimately dictate the long-term durability of MEMS components are critical in this maturing field.

The silicon-based films commonly used in micromechanical structures fall into the category of brittle structural materials and therefore inherit many of the traits, in particular low fracture toughness and damage tolerance, that preclude their use in conventional macro-scale applications. Research into the toughening of brittle structural materials, especially related to structural ceramics and intermetallics, has been extensive over the past couple of decades. The result is that there is now an extensive body of literature on how processing may be used to enhance the fracture toughness of these materials [1]. An unfortunate consequence of these (so-called extrinsic) toughening schemes, however, is that the material invariably becomes (more) susceptible to premature failure by fatigue when subjected to cyclic stresses [2].[1] Since it will be the damage tolerance, i.e. fracture and fatigue resistance, of the thin-film silicon that will most affect the reliability and long-term durability of MEMS

* Corresponding author. Tel.: +1-510-486-4584; fax: +1-510-486-4881.
E-mail address: cmuhlstn@uclink4.berkeley (C.L. Muhlstein).

[1] An example of this is the cyclic fatigue of polycrystalline ceramics, such as Al_2O_3, Si_3N_4 and SiC, which fail intergranularly and are thus toughened by the bridging of interlocking grains in the crack wake; under cyclic loading, frictional wear in the sliding interfaces can lead to a progressive degradation in the potency of these grain bridges, thereby effectively "detoughening" the material and causing premature (fatigue) failure [2].

0924-4247/01/$ – see front matter © 2001 Elsevier Science B.V. All rights reserved.
PII: S0924-4247(01)00709-9

devices, it is the objective of the current work to examine in detail the high-cycle fatigue behavior of 2 μm thick polycrystalline silicon films over lives of $\sim 10^5$ to 10^{11} cycles under high frequency (∼40 Hz) loading conditions.

2. Background

As insufficient mechanical strength can preclude the use of a material in structural applications, studies that have characterized the strength distribution of polycrystalline silicon are an important metric for design of micromechanical structures [3]. However, strength-based design approaches for MEMS are of limited practical value since our ability to apply large forces with existing actuator technologies is quite restricted. Similarly, studies that explore the fracture toughness of polycrystalline silicon give important insight into the damage tolerance of polycrystalline silicon and the largest flaws that may be tolerated in a given application [4]. However, in few cases the durability or long-term mechanical properties of thin-film polycrystalline silicon have been modified, or even examined, to the extent that has been carried out for the bulk forms of brittle structural materials. While probabilistic and fracture toughness-based design methodologies are important, the long-term durability of structures is ultimately limited by mechanisms such as fatigue that allow flaws to develop and/or existing flaws to grow.

The fatigue behavior of mono and polycrystalline silicon thin films has proven to be different from what would be expected based on the behavior of bulk brittle materials. Given the limited fracture toughness of silicon-based structural films and the apparent absence of "extrinsic" toughening mechanisms in the popular forms of structural silicon fabricated using low pressure chemical vapor deposition (LPCVD), one would not expect to observe cyclic fatigue in these thin films. In spite of this, thin silicon films have been shown to be susceptible to both fatigue crack growth in moist air [5,6], as well as to fatigue crack initiation [7–10]. Furthermore, fatigue degradation of actual silicon-based MEMS has even been observed [11]. Similar links between moisture and enhanced crack growth have also been reported for polycrystalline silicon thin films. However, much of the data has suffered from questionable accuracy in the stress amplitudes and/or times to failure and from the limited numbers of experiments conducted. Consequently, the objective of the current work was to generate a large body of carefully quantified, stress-life fatigue results for polycrystalline silicon in laboratory air and to examine the effect of modest variations in release conditions during processing. It is hoped that this fatigue characterization of polycrystalline silicon structural films will provide a useful resource for designers.

3. Materials and experimental procedures

3.1. Test techniques

The stress-life fatigue behavior of the polycrystalline silicon was investigated using the "structure" shown in Fig. 1. This micron-scale fatigue characterization structure is ∼300 μm square, and is analogous to a specimen, electromechanical load frame and capacitive displacement transducer found in a conventional mechanical testing system.

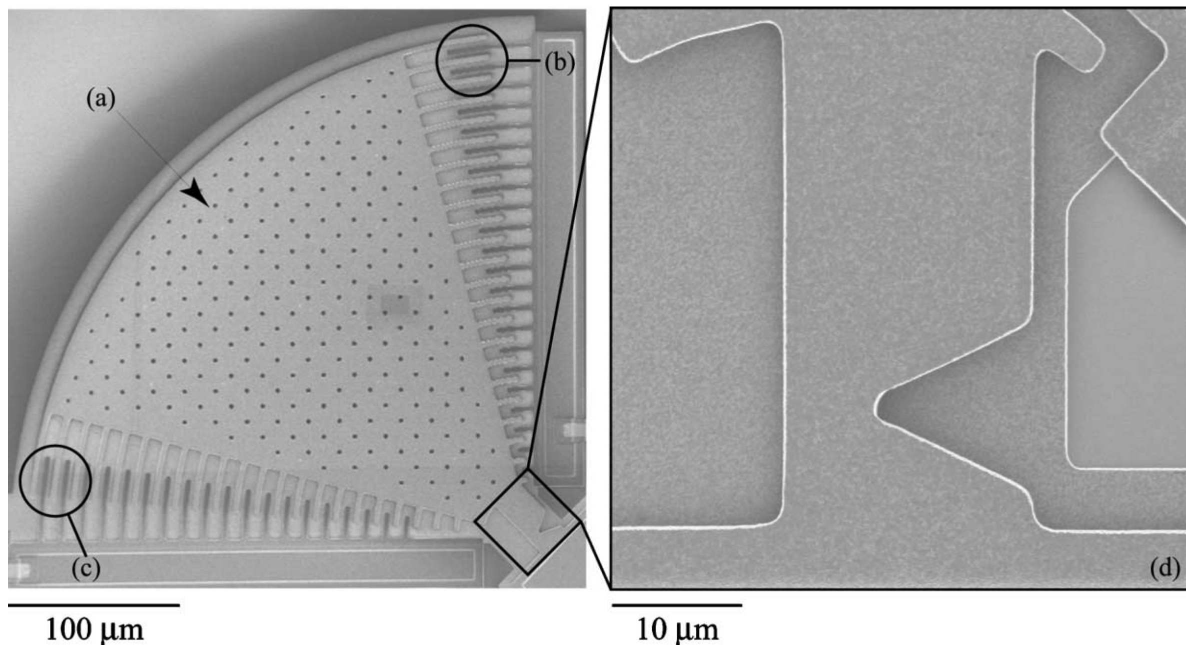

Fig. 1. Scanning electron micrographs of the fatigue life characterization structure used in this investigation. The (a) mass, (b) comb drive actuator, (c) capacitive displacement sensor and (d) notched cantilever beam (insert) are shown.

The specimen is a notched cantilever beam that is in turn attached to a large, perforated plate that serves as a resonant mass. The stress concentration in the form of a notch is introduced in the beam through the mask set used to define the surface micromachined structure. The mass and beam are electrostatically forced to resonate and the resulting motion is measured capacitively. On opposite sides of the resonant mass are interdigitated "fingers" commonly referred to as "comb drives". One side of these drives is for electrostatic actuation, while the other side provides capacitive sensing of motion. The specimen is attached to an electrical ground and a sinusoidal voltage with no dc offset at the appropriate frequency is applied to one comb drive, thereby inducing a resonant response in the plane of the figure. These conditions generate fully reversed, constant amplitude, sinusoidal stresses at the notch, i.e. a load ratio, R (ratio of minimum to maximum load) of -1, that are controlled to better than 1% precision. The opposing comb drive is attached to a constant potential difference and the relative motion of the grounded and biased fingers induces a current proportional to the amplitude of motion. The small induced current is converted to a dc voltage using an analog circuit. A variety of circuits for capacitive sensing can be found in [12]. The circuit output was proportional to the stress amplitude, $\sigma_a = (1/2)(\sigma_{max} - \sigma_{min})$, where σ_{max} and σ_{min} are the maximum and minimum stresses in the cycle, respectively.

The dynamic behavior of the fatigue characterization structure and the output of the capacitive motion sensing circuit were calibrated with the computer microvision system developed by Freeman and coworkers at the Massachusetts Institute of Technology (Cambridge, MA) [13]. Originally developed for transparent biological samples for hearing research, the system has been adapted for characterization of the opaque, higher frequency devices encountered in MEMS. The system consists of a light microscope, stroboscopic light source, charge coupled device (CCD) camera and a function generator whose operation is coordinated by a personal computer and custom-built timing hardware. If one assumes that the intensity of light reflected from an object is independent of its position, its motion can be found by comparing a time series of images using gradient-based machine vision algorithms developed by Horn [14–19]. This strategy allows the characterization of three-dimensional, periodic motion with a noise floor of better than 10 nm. This system was used to confirm that the motion of the fatigue characterization structure was sinusoidal and that it behaved as a rotational mass–spring oscillator that moved in the plane of Fig. 1. Out-of-plane motion due to the out-of-plane bending and torsional modes was not observed when the structure was excited at or near the in-plane bending resonant frequency, f_0. Similarly, the relationship between in-plane motion and the output of the capacitive sensing circuit was calibrated using computer microvision. Two structures were driven at resonance in the in-plane bending mode over a range of electrostatic force amplitudes and the resulting circuit output measured. At each drive amplitude, images were collected at eight evenly spaced phases of the electrostatic excitation. After two-point flat fielding [20,21] was used to reduce the effect of imperfections in the CCD array and optics of the system; the motion of three areas near the outer edge of the rotating mass was calculated. Reasonable agreement between the regions of interest on each structure and between the two samples was found. In order to determine the relationship between the measured motion of the structure and the amplitude of stresses in the vicinity of the notch, finite element methods were used.

The stress state in the vicinity of the notch was calculated using a commercial finite element package (ANSYS version 5.5). The fatigue characterization structure was modeled as an elastically isotropic, notched, cantilever beam and rigid mass with the geometry determined by scanning electron microscopy (SEM) of released devices. Eight node, plane-stress solid elements with constant thickness were used in the model and small elastic deformations were assumed. The mesh in the vicinity of the notch was refined until solutions to the model converged. An average of the Voigt and Reuss bounds for a random, polycrystalline aggregate (Young's modulus, $E = 163$ GPa, Poisson's ratio, $\nu = 0.23$ [22]) was used for the elastic properties of the elements. The Young's modulus measured from the resonant frequency of the fatigue structure was not used because current dynamic models underestimate E by $\sim$15% when compared to micro tensile and bulge testing data and calculations [3,23,24]. This conservative model neglects the elastic compliance of the anchor of the beam. Models of a cantilever beam attached to an elastic anchor show the upper bound of this error to be $\sim$5% [25]. The motion of the center of mass introduces a sinusoidally varying shear force, bending moment and axial force on the end of the cantilever beam. The relative magnitudes of the shear force and bending moment applied to the end of the notched cantilever beam were determined from the geometry of the structure and are largest at the maxima of the sinusoidally varying motion. In contrast, the axial force, F_{ax}, due to inertial effects is 0 at these maxima since $F_{ax} \propto (A\omega)^2 \cos^2(\omega t)$, where A is the rotational amplitude, ω the frequency and t time. Therefore, it has no impact on the maximum principal stresses in the beam. The maximum inertial force ($\sim 5.5 \times 10^{-6}$ N in short life tests) has a negligible effect on waveform since it only induces a maximum principal stress of $\sim$1 MPa at the root of the notch. Since the failure of brittle materials is often dictated by the maximum principal stress, the output of the sense circuit and finite element model described here were used to calculate the maximum principal stress amplitude at the notch. The accuracy of the stress amplitude calculated from the finite element model is ultimately limited by our understanding of the elastic modulus and boundary conditions of the fatigue characterization structure, but will have no bearing on the trends observed in the fatigue data.

The fatigue characterization structure was driven at resonance using the following control scheme. The first mode resonant response of the specimen was determined by sweeping a range of frequencies around the expected natural frequency and monitoring the output of the calibrated sense circuit. The peak amplitude was selected by fitting a second-order polynomial to the peak and extracting the maximum. The specimen was then excited at the peak frequency at a defined excitation voltage for about 1 to 5 min before reevaluating the resonant frequency. For this system, the peak amplitude is within about 10 parts-per-million (ppm) of the natural frequency of the structure and is used as the resonant frequency for control and analysis purposes. The change in resonant frequency with time was used to monitor the accumulation of fatigue damage in the specimen until failure occurred by complete separation at the notch. Baseline experiments using the fatigue characterization structure without a notch have established that changes in resonant frequency are a result of damage accumulation during fatigue and are not due to changes in temperature, relative humidity or accumulation of debris [6,25].

4. Materials, specimen preparation and testing environment

The specimens used in this study were fabricated from the first structural polysilicon layer on run 18 of the MCNC/Cronos MUMPs^{TM} process. This standard micromachining process for this foundry is based on the low pressure chemical vapor deposition (LPCVD) of n^+-type (resistivity, $\rho = 1.9\times 10^{-3}$ Ω cm) polycrystalline silicon [26]. The nominally 2 μm thick films from this process are usually described as having a columnar microstructure with grain diameters in the order of 0.1 μm [27]. A plan view of the polycrystalline silicon microstructure used in this study is shown in Fig. 2. No

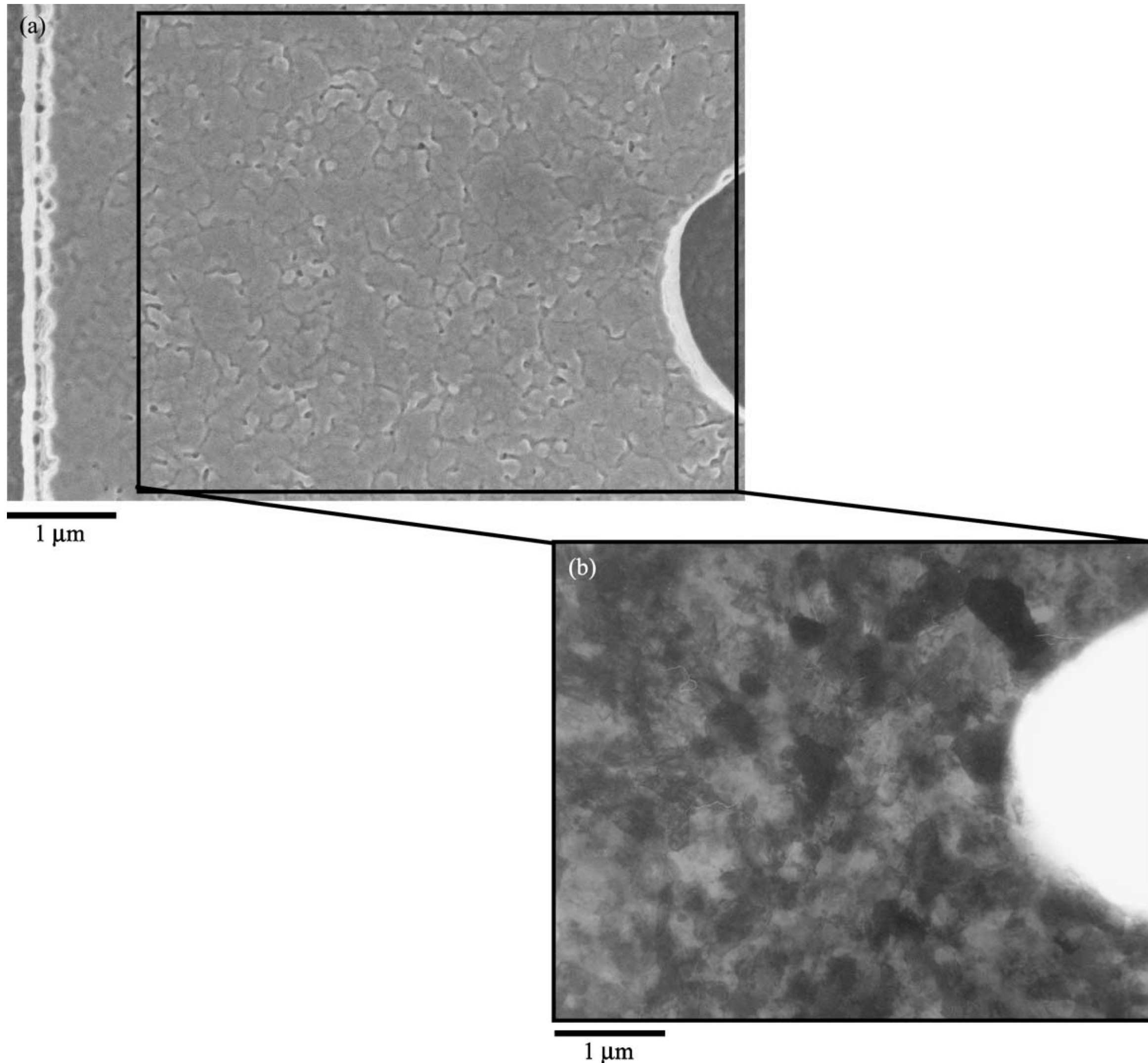

Fig. 2. (a) Scanning electron micrograph and (b) high voltage transmission electron micrograph of the polycrystalline silicon used in this study. The grain size is relatively uniform, even in the vicinity of features such as the notch root shown on the right side of the micrographs.

variations in microstructure in the vicinity of features such as the root of the notch in the cantilever beam were observed. Wafer curvature measurements showed the structural layer in the film to have a compressive residual stress of about 9 MPa [26]; out-of-plane deformation due to a through-thickness residual stress gradient in the film could not be detected using white light interferometry. Secondary ion mass spectroscopy (SIMS) was used to quantify the concentration of hydrogen, carbon, oxygen and phosphorous present in the structural films in this investigation. The interior of the polysilicon film contained $\sim 1 \times 10^{19}$ atoms/cm^3 phosphorous, 2×10^{18} atoms/cm^3 hydrogen, 1×10^{18} atoms/cm^3 oxygen and 6×10^{17} atoms/cm^3 carbon. Concentrations were quantified using standards of known composition and are accurate to better than 20%. The presence of significant amounts of hydrogen, oxygen and carbon are consistent with the deposition technique and the thermal history of the film. The high concentration of phosphorous is consistent with the measured resistivity of the material and with the fact that phosphosilicate glass was used to dope the structural film.

The notched cantilever beam specimen used in this investigation is shown schematically in Fig. 3. The notched beams were designed for testing at ~40 kHz and were ~40 μm long, 19.5 μm wide and 2 μm thick. The notch was located 9.8 μm from the base and was 13 μm deep. The notch root radius was ~1 μm and represents the smallest root radius that could be created given the processing conditions. Two groups of samples were prepared for testing by first removing the sacrificial oxide layer in 49% hydrofluoric acid for 2.5 and 3 min, respectively. After drying at 110°C in air, the samples were mounted in ceramic electronic packages and ultrasonically wire bonded for testing. Prior to fatigue testing, every structure was run for 15 min ($\sim 35 \times 10^6$ cycles) at ~450 MPa to verify system electrical performance and screen for abnormalities that may have arisen in fabrication, release, packaging or handling. The specimens were then tested until failure in laboratory air (nominally 25°C,

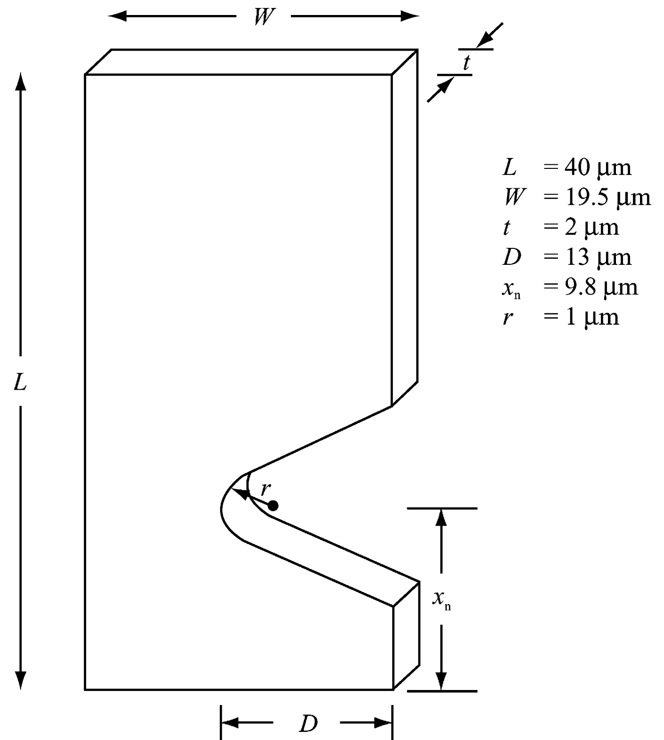

Fig. 3. Schematic of the cantilever beam geometry used in this investigation.

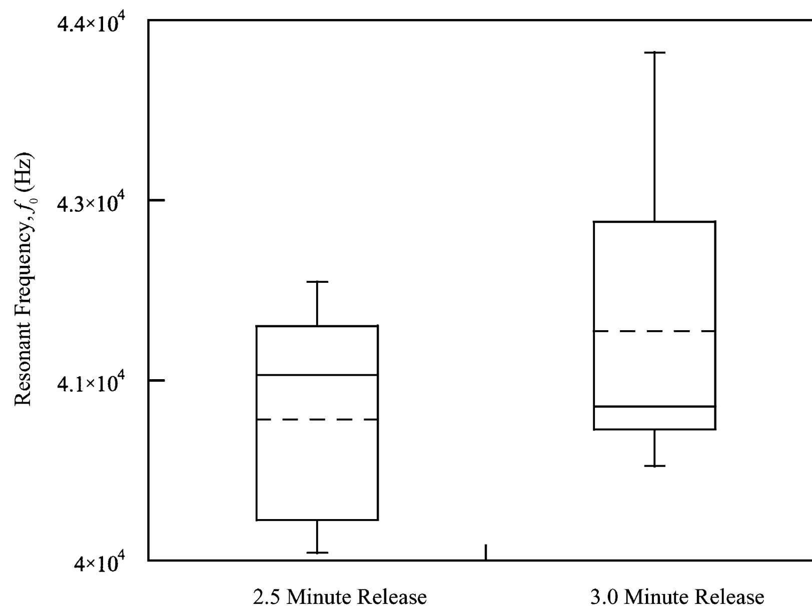

Fig. 4. "Box plot" comparison of the resonant frequency of 22 structures released for 2.5 min and 14 structures released for 3.0 min. The resonant frequency was characterized at a stress amplitude of about 450 MPa. The top and bottom of the box are the upper and lower quartiles, the solid horizontal line denotes the median value, the dashed horizontal line denotes the mean value and the error bars denote the maximum and minimum values of the data.

30–50% relative humidity) using the previously described control scheme.

A total of 28 fatigue specimens were tested until failure in laboratory air with lives, N_f, ranging from about 10 s to 34 days (3×10^5 to 1.2×10^{11} cycles) over fully reversed, sinusoidal stress amplitudes ranging from ~2.0 to 4.0 GPa. Fifteen of the samples were exposed to hydrofluoric acid for 2.5 min during the release procedure and the remaining 13 samples were released for 3 min. The variability in dimensions, especially film thickness, typically leads to a measurable variation in the resonant frequency of surface micromachined devices. Despite this variability, the effect of the 20% increase in etch time was observed in the mean natural frequency of the samples measured at a stress amplitude of about 450 MPa (Fig. 4). After testing, the crack path and fracture surfaces of the specimens were characterized using scanning electron microscopy (SEM).

5. Results and discussion

Results from the stress-life testing of the thin film polycrystalline silicon cantilever beams are shown in Fig. 5. Samples exhibited a time-delayed failure when subjected to fully reversed, sinusoidal, cyclic stresses in relatively moist, room temperature air. This apparent cyclic fatigue effect resulted in an endurance strength, at greater than 10^9 cycles, of ~2 GPa, i.e. roughly one-half of the (single cycle) fracture strength. We have found similar behavior for slightly thicker (20 μm) films of single crystal silicon [9].

The 15 specimens subjected to a 2.5 min release in hydrofluoric acid displayed fatigue lives ranging from ~25 s to 12 days (1×10^6 to 4.5×10^{10} cycles) over stress amplitudes ranging from about 2.6 to 3.5 GPa. Similarly, the 13 polycrystalline silicon specimens released for 3 min exhibited lives ranging from about 10 s to 34 days (3×10^5 to 1.2×10^{11} cycles) before failure over stress amplitudes ranging from ~2.2 to 3.0 GPa. No significant effect of release time was observed. The peak tensile stress in the short life tests was similar to the single cycle fracture or ultimate, strength usually measured in polycrystalline silicon [3]. Typically, delayed failures of brittle materials in stress-life tests will be clustered around this stress level. The life of the thin film polycrystalline silicon, however, increased monotonically with decreasing stress amplitude with a 50% reduction in stress amplitude resulting in an increase in life of approximately five orders of magnitude. This trend has not been observed in the fatigue stress-life testing of any bulk brittle materials (e.g. [28]); instead, a range of lives close to the strength of the material is usually observed with few delayed failures at lower stress amplitudes.

The resonant frequency of the cantilever beam was used to monitor the specimen during cyclic loading and was observed to decrease monotonically before the specimen finally failed from the notch (Fig. 6). The change in compliance of the notched beam induced a decrease in resonant frequency that ranged from undetectable to over 50 Hz in the long life tests. This change in natural frequency is defined as $f_f - f_0$, where f_f and f_0 are the resonant frequencies at failure and the start of the test, respectively. This behavior strongly suggests that the failure of the thin film polycrystalline silicon occurs after progressive accumulation of damage, e.g. by the stable propagation of a crack.

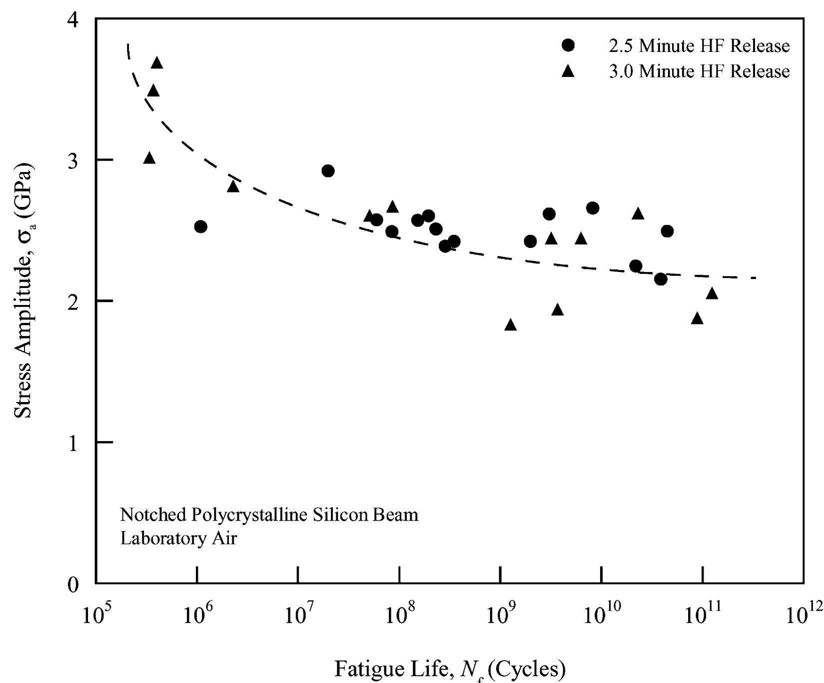

Fig. 5. Stress-life (S/N) fatigue data for polycrystalline silicon in laboratory air. Specimens released for 2.5 and 3.0 min display similar fatigue lives.

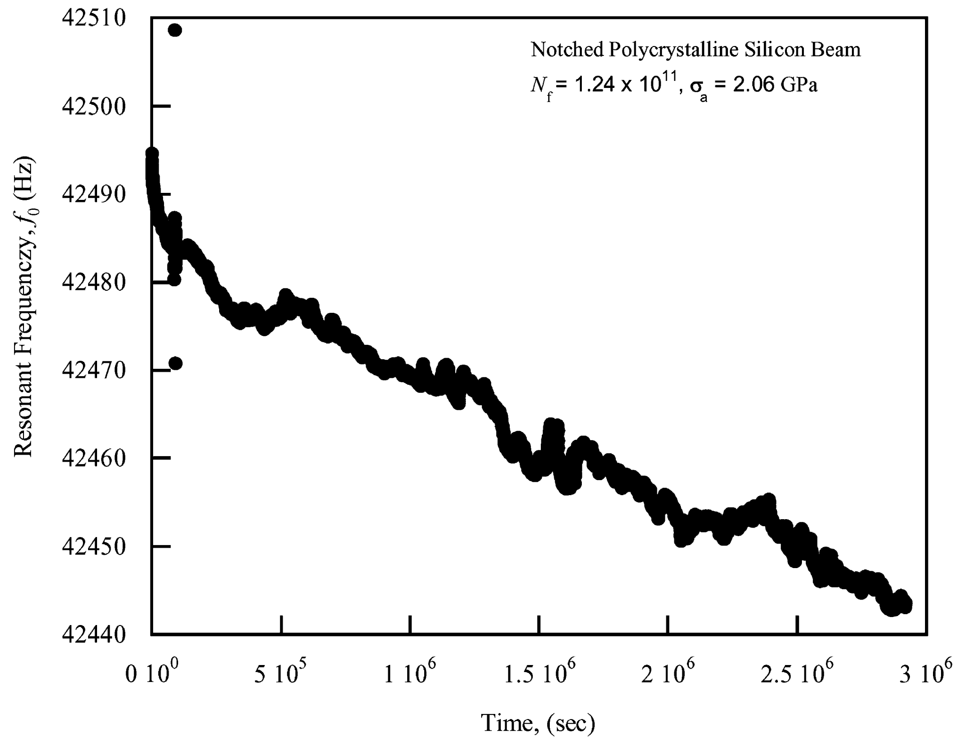

Fig. 6. Resonant frequency as a function of time during fatigue testing ($N_f = 1.24 \times 10^{11}$ cycles at $\sigma_a = 2.06$ GPa).

This manifests itself as a progressive decay in the stiffness (resonant frequency) of the cantilever beam. The longer the life of the specimen, the larger the decrease in beam stiffness (Fig. 7), which is again consistent with the notion of the accumulation of damage. The link between the change in resonant frequency and the fatigue process have been investigated using finite element methods.

Although one can anticipate that the details of the microstructure, residual stresses and post-processing will have important effects on the actual stress-life behavior, the

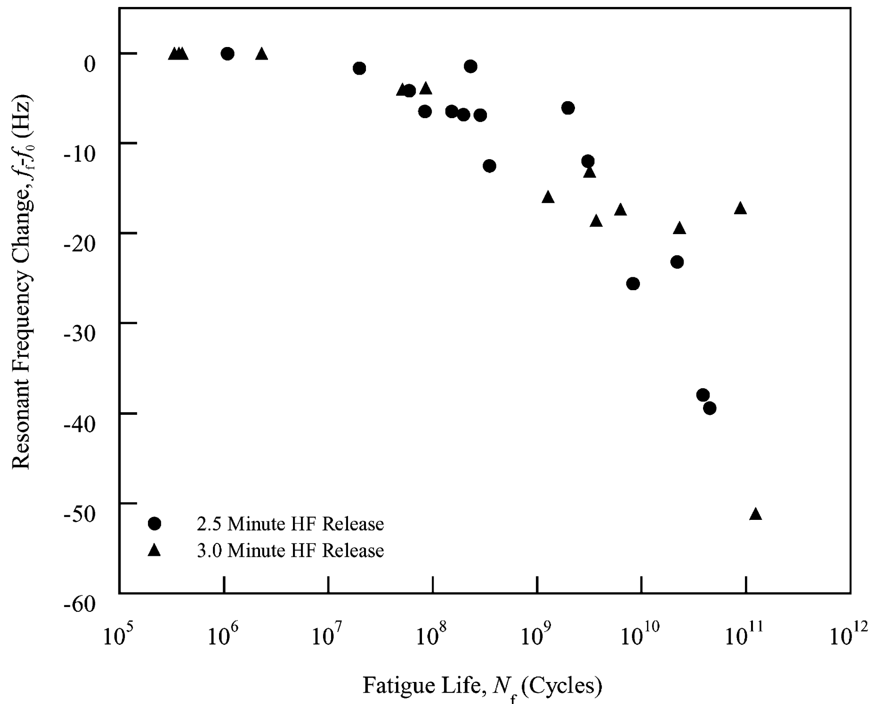

Fig. 7. Change in resonant frequency ($f_f - f_0$) as a function of specimen life for stress-life samples shown in Fig. 5.

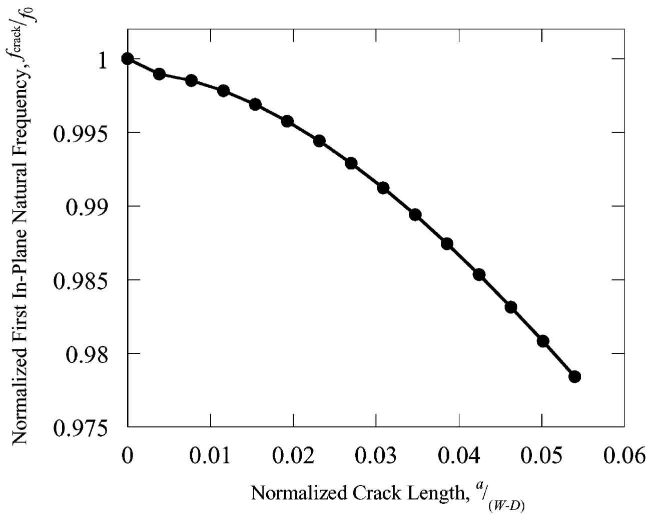

Fig. 8. Normalized change in natural frequency (f_{crack}/f_0) as a function of normalized crack length, $a/(W-D)$. f_{crack} and f_0 are the in-plane resonant frequencies of the cracked and crack-free, notched structures and the crack length, a, is normalized with respect to the remaining ligament of the notched beam $(W-D)$ as defined in Fig. 3.

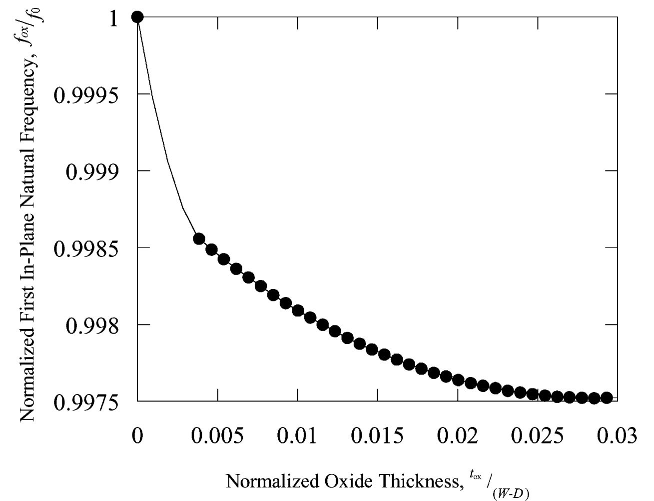

Fig. 9. Normalized change in natural frequency (f_{crack}/f_0) as a function of normalized oxide thickness, $t_{ox}/(W-D)$. f_{ox} and f_0 are the in-plane resonant frequencies of the oxidized and oxide-free, notched structures and the oxide thickness, t_{ox}, is normalized with respect to the remaining ligament of the notched beam $(W-D)$ as defined in Fig. 3.

fatigue susceptibility of polycrystalline silicon thin films must be associated with some local damage phenomena. Neither of the recognized fatigue damage mechanisms for ductile and brittle materials, i.e. dislocation activity to cause alternating blunting and resharpening of the crack tip and cycle-dependent degradation in crack-tip shielding in the crack wake [2], respectively, appear to be relevant to single crystal and polycrystalline silicon films. Two possible origins of the change in resonant frequency are localized cracking and oxidation at the root of the notch. Plane stress finite element modal analyses were performed using ANSYS to evaluate the effect of localized cracking and oxidation on the natural frequency of the fatigue characterization structure. The model of the cracked, notched fatigue structure used six-node, triangular, plane stress elements with constant thickness and material properties identical to those used in the stress analysis described previously. The singularity at the crack tip was modeled with 12 circumferential, unskewed elements 1/20 of the crack length in size. The remaining element size was refined until model

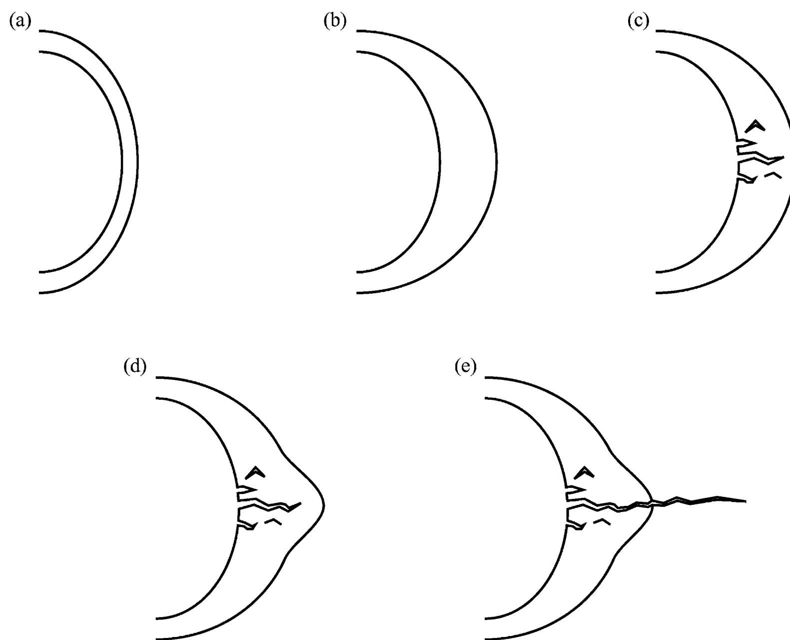

Fig. 10. Schematic of the reaction layer fatigue mechanism at the root of the notch. (a) Reaction layer (native oxide) on surface of the silicon, (b) localized oxide thickening at the notch root, (c) stress corrosion cracking of the notch root, (d) additional thickening and cracking of reaction layer and (e) critical crack growth in the silicon film.

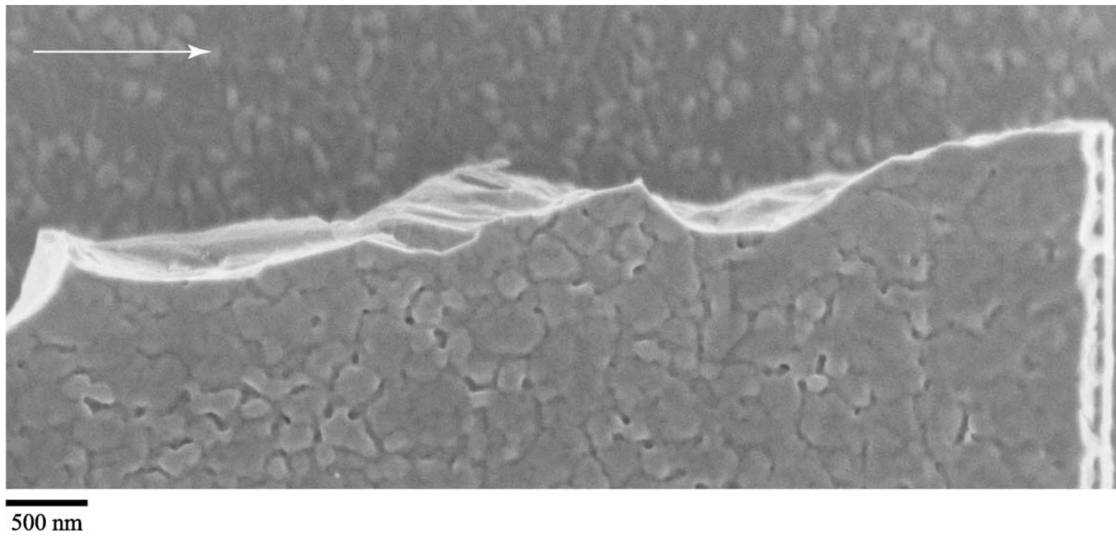

Fig. 11. Scanning electron micrograph of the crack profile of a short life fatigue test (1.1×10^6 cycles at $\sigma_a = 3.04$ GPa). The arrow indicates the direction of crack propagation.

convergence was achieved. The in-plane natural frequencies and mode shapes were determined using the subspace iteration routines available in the finite element code. The model suggests that for $\sim$1 nm of crack extension a 1 Hz change in natural frequency should be observed (Fig. 8). To model the effect of local oxidation at the notch root, the surface of the notch root was dilated and the material properties changed to those of bulk SiO_2 ($E \approx 60$ GPa,

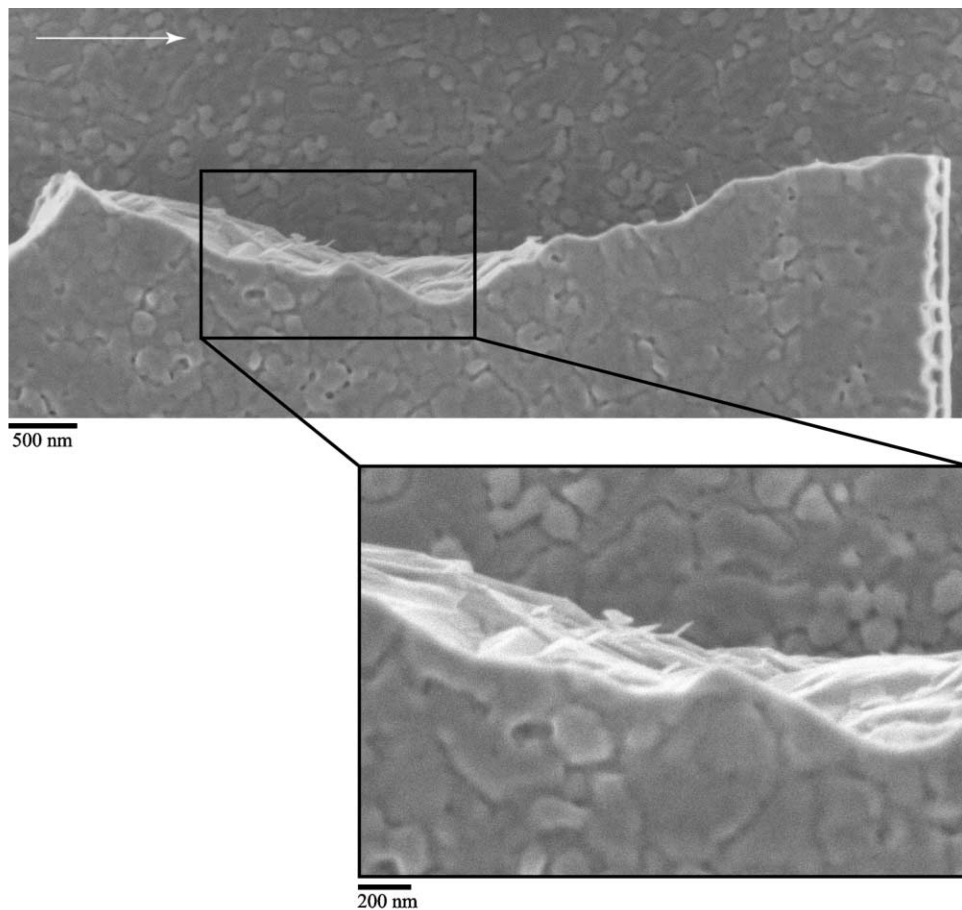

Fig. 12. Scanning electron micrograph of the crack profile of a long life fatigue test (3.8×10^{10} cycles at $\sigma_a = 2.59$ GPa). The arrow indicates the direction of crack propagation. Detail shows the fine, needle-like features and debris on the fracture surface.

$v \approx 0.2$). The $Si–SiO_2$ interface was placed 46% of the oxide thickness into the silicon structural film to model the loss of silicon during the oxidation process. Although the cross section of the cantilever beam increases, the presence of the relatively low elastic modulus SiO_2 results in an initial decrease in the natural frequency with increasing oxide layer thickness (Fig. 9). This occurs at a rate very similar to cracking; a 1 nm increase in oxide thickness leads to about a 0.5 Hz decrease in the resonant frequency. These finite element models suggest that both phenomena are consistent with the experimentally observed changes in the natural frequency. Furthermore, the changes in resonant frequency are consistent with processes occurring on length scales commensurate with the native oxide thickness. Based on these numerical results, we propose the following mechanism for fatigue crack initiation in silicon.

Fatigue cracks are believed to initiate in silicon during the local oxidation and stress corrosion cracking of the native SiO_2 layer on the silicon via a mechanism that we term reaction-layer fatigue. The sequence of events in the crack initiation process are shown in Fig. 10 and described as follows. Upon initial contact with air, the native oxide reaction layer forms on the silicon and the thickness is dictated by the temperature, relative humidity and duration of the exposure. Then, during fatigue loading, the oxide at the root of the notch locally thickens due to the thermomechanical driving forces. Cracks then form since this oxide is susceptible to stress corrosion cracking. Subsequent crack extension and final failure may then occur via continued local oxidation and stress corrosion cracking. This type of fatigue mechanism is quite general and need not be limited to silicon-based films. Presently, experiments are underway to directly evaluate local oxidation and cracking processes that may occur at the root of the notch during fatigue loading.

Fractography of the fatigue specimens using low voltage SEM was used to establish the mode of crack advance and its interaction with the microstructure of the polycrystalline silicon film without altering the surfaces by coating with

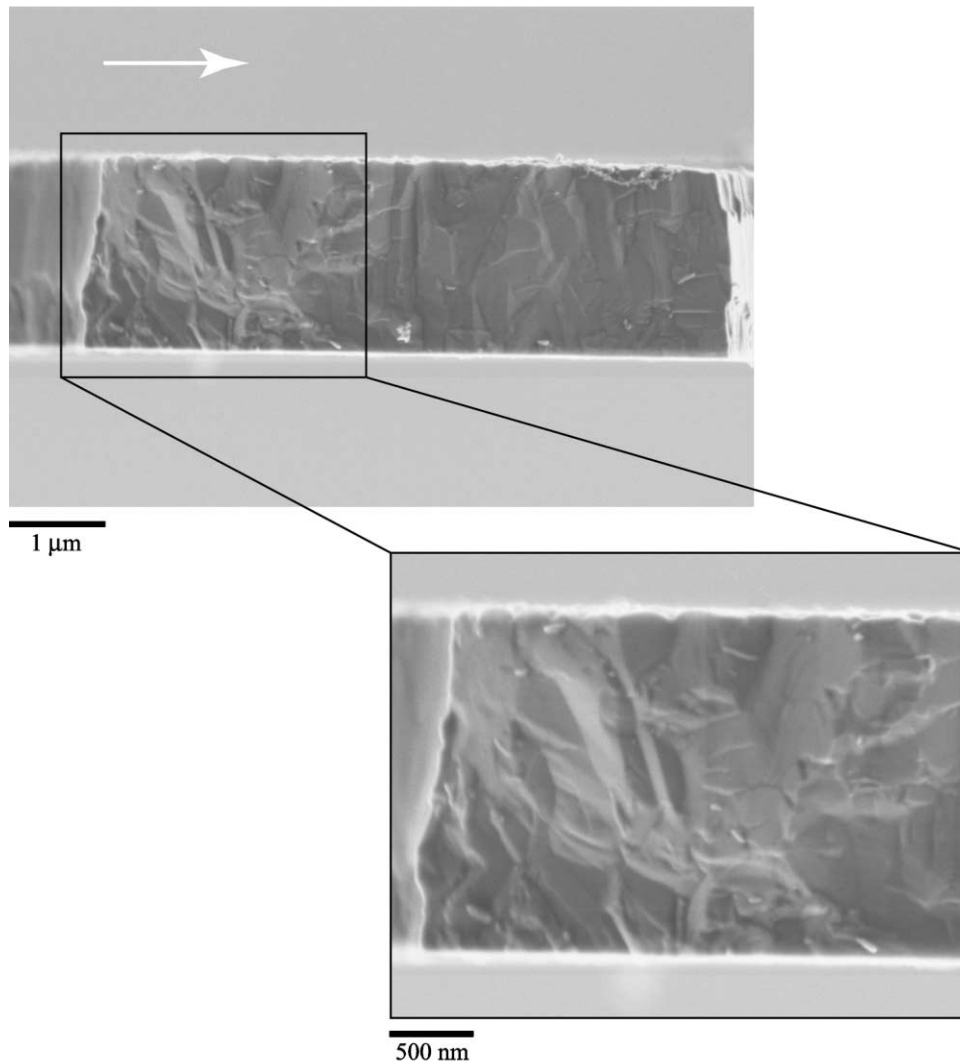

Fig. 13. Scanning electron micrograph of a fracture surface of specimen shown in Fig. 12 ($N_f = 3.8 \times 10^{10}$ cycles at $\sigma_a = 2.59$ GPa). The arrow indicates the direction of crack propagation.

conductive layers such as carbon or gold–palladium alloys. The crack paths were transgranular in both short (Fig. 11) and long life (Fig. 12) fatigue tests. The crack was observed to meander both through the thickness of the film and along the remaining ligament of the notched beam. It is unclear if the crack path is influenced by the residual stresses or details of the microstructure of the film. In both short and long life specimens, interesting fine features were observed on the fracture surfaces. Needle-like slivers and other debris were found on the fracture surface that would be consistent with distributed damage in the film or the presence of unidentified secondary phases based on impurities such as oxygen and carbon. Direct observation of the fracture surface of the failed samples revealed the relatively featureless surfaces as shown in Fig. 13. The presence of ridges, cusps, river markings and other features are consistent with the brittle nature of the polycrystalline thin film. Similar features have been reported for the fracture behavior of mono and polycrystalline silicon; [9,29,30] however, unlike these investigations, no discrete region denoting crack initiation was visible. Consequently, the fracture surface morphology provided only limited insight into the initial flaw that propagated to failure during the fatigue test.

From the perspective of the relevance of stress/life data for engineering design and durability, two classes of fatigue-related problems may be of concern for designers of polysilicon MEMS devices. First, the component performance may degrade due to the loss in stiffness associated with fatigue damage. This is an important consideration for ensuring the performance of filters and other timing-critical devices as well as sensors such as accelerometers that rely on the invariance of the compliance of the structure. Second, polysilicon devices subjected to cyclic stresses are susceptible to premature failure by fatigue. In fact, the data in this study confirm that the use of a strength-based design approach for MEMS will not prevent the premature failure of a cyclically loaded structure at stresses as low as 50% of the (tensile) strength of the material. Clearly, the availability of stress-life fatigue data and an understanding of the fatigue mechanism(s) for MEMS materials remain important to improving the performance of these devices and to evaluating their long-term durability.

6. Conclusions

Based on an experimental study of the cyclic fatigue behavior of thin (~2 μm) films of polycrystalline silicon at high frequencies (~40 kHz) in laboratory air, the following primary conclusions can be made:

- Similar to previously reported data for 20-μm thick single crystal silicon films, 2 μm thick polysilicon films can degrade and fail under cyclic loading conditions in moist, ambient air at cyclic stresses some 50% of the single cycle fracture strength.
- Numerical models suggest that damage accumulation during fatigue crack initiation is a surface phenomenon related to both surface oxidation and cracking. This is consistent with the notion of a mechanism for the premature fatigue of thin silicon films involving reaction-layer fatigue.
- Fatigue failure of thin silicon films at stresses much lower than their fracture strength may be a significant limitation to the long-term frequency stability, reliability and life of polycrystalline silicon micromechanical devices. Even if a structure made from silicon does not fail, the loss of stiffness may lead to a large accumulated error that may detrimentally affect the components that rely on a constant stiffness for timing or inertial measurement (i.e. an oscillator or gyroscope).

Acknowledgements

This work was supported by a grant from Exponent Inc. to the University of California. Additional support to one of the authors (S.B. Brown) was provided by DARPA. The authors wish to thank Werner Hemmert, A.J. Aranyosi and D. Freeman (MIT) for assistance with computer microvision, W. Van Arsdell (Exponent Inc.) for the original specimen design and layout and E.A. Stach (National Center for Electron Microscopy, Lawrence Berkeley National Laboratory) for help with the high-voltage transmission electron microscopy.

References

[1] A.G. Evans, Perspective on the development of high-toughness ceramics, J. Am. Ceram. Soc. 73 (1990) 187–206.

[2] R.O. Ritchie, Mechanisms of fatigue-crack propagation in ductile and brittle solids, Int. J. Fract. 100 (1999) 55–83.

[3] W.N. Sharpe Jr., S. B. Brown, G.C. Johnson, W. Knauss, Round-robin tests of modulus and strength of polysilicon, Microelectromechanical Structures for Materials Research, San Francisco, CA, 1998, pp. 57–65.

[4] H. Kahn, N. Tayebi, R. Ballarini, R.L. Mullen, A.H. Heuer, Fracture toughness of polysilicon MEMS devices, in: Proceedings of the 10th International Conference on Solid State Sensors and Actuators (Transducers '99), Sendai, Japan, 1999, pp. 274–280.

[5] J.A. Connally, S.B. Brown, Slow crack growth in single-crystal silicon, Science 256 (1992) 1537–1539.

[6] W.W. Van Arsdell, S.B. Brown, Subcritical crack growth in silicon MEMS, J. Microelectromechanical Syst. 8 (1999) 319–327.

[7] S.B. Brown, W.W. Van Arsdell, C.L. Muhlstein, Materials reliability in MEMS devices, Proceedings of International Solid State Sensors and Actuators Conference (Transducers '97), Chicago, IL, USA, 1997, pp. 591–593.

[8] C.L. Muhlstein, S.B. Brown, Reliability and fatigue testing of MEMS, Tribology issues and opportunities in MEMS, in: Proceedings of the NSF/AFOSR/ASME Workshop on Tribology Issues and Opportunities in MEMS, Columbus, OH, USA, 1997, p. 80.

[9] C.L. Muhlstein, S.B. Brown, R.O. Ritchie, High-Cycle Fatigue of single crystal silicon thin films, J. Microelectromechanical Syst. (2001) in press.

[10] H. Kahn, R. Ballarini, R.L. Mullen, A.H. Heuer, Electrostatically actuated failure of microfabricated polysilicon fracture mechanics specimens, Proc. Royal Soc. London A 455 (1999) 3807–3823.
[11] T. Tsuchiya, A. Inoue, J. Sakata, M. Hashimoto, M. Sugimoto, Fatigue Test of Single Crystal Silicon Resonator, in: Proceedings of the 16th Sensor Symposium, 1998, pp. 277–280.
[12] L.K. Baxter, Capacitive sensors: design and applications, IEEE Press, New York, 1997.
[13] D.M. Freeman, A.J. Aranyosi, M.J. Gordon, S.S. Hong, Multidimensional motion analysis of MEMS using computer microvision, Solid-State Sensor and Actuator Workshop Technical Digest, Solid-State Sensor and Actuator Workshop, Hilton Head Island, SC, USA, 1998, pp. 150–155.
[14] B.K.P. Horn, Robot Vision, MIT Press, Cambridge, MA, 1986.
[15] B.K.P. Horn, E.J. Weldon Jr., Direct methods for recovering motion, Int. J. Comput. Vision 2 (1988) 51–77.
[16] C.Q. Davis, D.M. Freeman, Statistics of subpixel registration algorithms based on spatiotemporal gradients or block matching, Opt. Eng. 37 (1998) 1290–1298.
[17] C.Q. Davis, D.M. Freeman, Using a light microscope to measure motions with nanometer accuracy, Opt. Eng. 37 (1998) 1299–1304.
[18] S. Timoner, Subpixel motion estimation from sequences of video images, Electrical Engineering and Computer Science, MIT Press, Cambridge, MA, 1999.
[19] S. Timoner, D.M. Freeman, Multi-image gradient-based algorithms for motion estimation, Optical Eng., 2001, in press.
[20] Y. Hiraoka, J.W. Sedat, D.A. Agard, The use of a charge-coupled device for quantitative optical microscopy of biological structures, Science 238 (1987) 36–41.
[21] G.E. Healey, R. Kondepudy, Radiometric CCD camera calibration and noise estimation, IEEE Trans. Pattern Anal. Machine Intelligence 16 (1994) 267–276.
[22] G. Simmons, H. Wang, Single crystal elastic constants and calculated aggregate properties, A Handbook, 2nd Edition, MIT Press, Cambridge, MA, 1971.
[23] W.N. Sharpe Jr., K.T. Turner Jr., R.L. Edwards, Tensile testing of polysilicon, Experimental Mechanics 39 (1999) 162–170.
[24] S. Jayaraman, R.L. Edwards, K.J. Hemker, Relating mechanical testing and microstructural features of polysilicon thin films, J. Mater. Res. 14 (1999) 688–697.
[25] W. Van Arsdell, Subcritical Crack Growth in Polysilicon MEMS, Mechanical Engineering, Massachusetts Institute of Technology, Cambridge, MA, 1997.
[26] MCNC/Cronos, www.memsrus.com, 2000.
[27] W.N. Sharpe Jr., B. Yuan, R.L. Edwards, Fracture Tests of Polysilicon Film, in: Proceedings of the ASME International Mechanical Engineering Congress and Exposition Proceedings of 1997 International Mechanical Engineering Congress and Exposition, Applications of Experimental Mechanics of Electronic Packaging, Dallas, TX, USA, 1997, pp. 113–116.
[28] R.O. Ritchie, R.H. Dauskardt, Cyclic fatigue of ceramics: a fracture mechanics approach to subcritical crack growth and life prediction, J. Ceram. Soc. Jpn. 99 (1991) 1047–1062.
[29] C.P. Chen, M.H. Leipold, Fracture toughness of silicon, Am. Ceram. Soc. Bull. 59 (1980) 469–472.
[30] F. Ebrahimi, L. Kalwani, Fracture anisotropy in silicon single crystal, Mater. Sci. Eng. A 268 (1999) 116–126.

Biographies

Christopher L. Muhlstein is a doctoral student in the Department of Materials Science and Engineering at the University of California, Berkeley. He received his BS in materials science and engineering from UC Berkeley (1994) and his MS in metallurgy from the Georgia Institute of Technology (1996). Mr. Muhlstein is the chair of ASTM task group E08.05.03 on Mechanical Properties of Structural Films for Micromechanical and Electronic Applications. His primary research interests are fracture and fatigue of structural materials.

Stuart B. Brown is the head of the Boston Office and principal of Exponent Inc. Dr. Brown received his BS in mechanical engineering from Washington University (1977), MS in mechanical engineering from Stanford University (1980) and PhD in mechanical engineering from MIT (1987). Dr. Brown is a member of Tau Beta Pi, Phi Beta Kappa, Pi Tau Sigma and Omicron Delta Kappa. His current research interests are in MEMS reliability.

Robert O. Ritchie is a professor in the Materials Science and Engineering Department at the University of California at Berkeley and the Head of Structural Materials in the Materials Sciences Division of the Lawrence Berkeley National Laboratory. Dr. Ritchie received his BA in physics and metallurgy (1969), MA in materials science (1973), PhD in materials science (1973) and DSc in materials science (1990), all from Cambridge University, UK. Dr. Ritchie is a member of the National Academy of Engineering and his primary research interest is in the mechanical behavior of materials.